

AD-A054 413

NAVAL RESEARCH LAB WASHINGTON D C
A GENERAL TWO-DIMENSIONAL TOKAMAK MODEL.(U)
MAR 78 M EMERY, J GARDNER, M FRITTS, J BORIS
NRL-MR-3744

F/G 18/1

UNCLASSIFIED

DOE-E(49-20)-1006
NL

[OF]

AD
A054413



END
DATE
FILMED
6 -78
DDC

FOR FURTHER TRAN

H. *12*

NRL Memorandum Report 3744 *SC*

AD A 054413

A General Two-Dimensional Tokamak Model

MARK EMERY

*Science Applications, Inc.
McLean, Virginia 22101*

and

JOHN GARDNER, MARTIN FRITTS, JAY BORIS and NIELS WINSOR

*Plasma Dynamics Branch
Plasma Physics Division*

AD No. ~~AD A 054413~~
DC FILE COPY

March 1978

This research was sponsored by the U.S. Dept. of Energy under Contract No. E(49-20)-1006



NAVAL RESEARCH LABORATORY
Washington, D.C.

DDC
RECEIVED
MAY 30 1978
D

SECURITY CLASSIFICATION OF THIS PAGE (When Data Entered)

REPORT DOCUMENTATION PAGE		READ INSTRUCTIONS BEFORE COMPLETING FORM	
1. REPORT NUMBER NRL Memorandum Report 3744 ✓ (14)		2. AUTHOR, TITLE, AND REPORT NUMBER (14) NRL-MR-3744	
4. TITLE (and Subtitle) (6) A GENERAL TWO-DIMENSIONAL TOKAMAK MODEL		3. PERIOD COVERED (9) Interim report on a continuing NRL problem.	
7. AUTHOR(S) (10) Mark Emery, John Gardner, Martin Fritts, Jay Boris Niels Winsor		5. PERFORMING ORG. REPORT NUMBER	
9. PERFORMING ORGANIZATION NAME AND ADDRESS Naval Research Laboratory Washington, D. C. 20375		8. CONTRACT OR GRANT NUMBER(s)	
11. CONTROLLING OFFICE NAME AND ADDRESS U.S. Department of Energy Washington, D.C. 20305		10. PROGRAM ELEMENT PROJECT, TASK AREA AND WORK UNIT NUMBERS (15) NRL Problem H02-27 Project DOE-E(49-20)-1006	
14. MONITORING AGENCY NAME & ADDRESS (if different from Controlling Office)		13. NUMBER OF PAGES (11) Mar 1978 (12) 25 p.	
		15. SECURITY CLASS. (of this report) UNCLASSIFIED	
16. DISTRIBUTION STATEMENT (of this Report) Approved for public release; distribution unlimited.		15a. DECLASSIFICATION/DOWNGRADING SCHEDULE	
17. DISTRIBUTION STATEMENT (of the abstract entered in Block 20, if different from Report)			
18. SUPPLEMENTARY NOTES This research was sponsored by the U.S. Department of Energy, Project No. E(49-20)-1006.			
19. KEY WORDS (Continue on reverse side if necessary and identify by block number) Nuclear fusion Triangular coordinates Computer model Tokamak Doublet			
20. ABSTRACT (Continue on reverse side if necessary and identify by block number) A two dimensional dynamic transport code has been developed. It assumes axisymmetry, but it is capable of modeling multiple magnetic axes, divertors and other complex geometries. A triangular mesh allows detailed analysis of separatrices, divertors and regions unstable to trapped-particle and ballooning modes.			

DD FORM 1 JAN 73 1473

EDITION OF 1 NOV 65 IS OBSOLETE
S/N 0102-014-6601

SECURITY CLASSIFICATION OF THIS PAGE (When Data Entered)

251 950

all

CONTENTS

INTRODUCTION 1
MATHEMATICAL MODEL 2
GEOMETRODYNAMICS 4
MAGNETOHYDRODYNAMICS 5
INITIAL CONDITIONS 10
TRANSPORT 11
SUMMARY AND CONCLUSIONS 13

ACCESSION for	
RTIS	White Section <input checked="" type="checkbox"/>
DDC	Buff Section <input type="checkbox"/>
UNANNOUNCED	<input type="checkbox"/>
JUSTIFICATION.....	
BY.....	
DISTRIBUTION/AVAILABILITY CODE	
Dist.	AVAIL. and/or SPECIAL
A	

PRECEDING PAGE BLANK-NOT FILMED

A GENERAL TWO-DIMENSIONAL TOKAMAK MODEL

INTRODUCTION

This report describes a fully two-dimensional computer simulation model of tokamak discharges. This Lagrangian computer model is used to investigate the time evolution of a finite-conductivity plasma in a finite-conductivity vessel, based on the quasi-static evolution of pressure balance in the plasma. The code is unique in that it is designed so as to follow both the resistive diffusion and the gross dynamics of the plasma.

The Lagrangian coordinate system uses a general-connectivity triangular grid which permits an investigation of problems of much greater complexity than conventional, one-dimensional schemes. As examples, non-circular plasmas (elliptical or D-shaped), multiple magnetic axes including separatrices, and magnetic diverters can be described with this code. For a typical tokamak configuration, the plasma is represented by a series of concentric rings of vertex points. These rings are made to coincide with flux surfaces in the quasi-static approximation. The triangle sides connect points along these rings. More complicated geometries are just extensions of this basic scheme.

Figure 1 illustrates the ease with which a triangular mesh system can accommodate tokamak features such as limiters and conducting walls. The objective of this model is to treat dynamics in general configurations, including multipoles and separatrices, as in Fig. 2.

The present model is based on the assumption that the quasi-static pressure balance equation ($\nabla p = (1/c) \underline{j} \times \underline{B}$) is always satisfied. The equations are solved in an iterative manner, which removes the high-phase-velocity magnetosonic and Alfvén modes from consideration. Since we are interested in the long time-averaged behavior of this transport model, these waves are not of interest.

Note: Manuscript submitted February 22, 1978.

The model incorporates the diffusive fluxes of material, energy and magnetic fields.

In the next section we present the mathematical model. The details of the iterative approach to force balance are discussed in the subsequent sections.

MATHEMATICAL MODEL

The physical system of interest is the cross-section of a toroidal conducting shell and numerous current filaments. The shell contains a plasma and vacuum regions. The fields satisfy Maxwell's equations:

$$\underline{\nabla} \cdot \underline{E} = 0 \quad (1)$$

$$\underline{\nabla} \times \underline{E} = -\frac{1}{c} \frac{\partial \underline{B}}{\partial t} \quad (2)$$

$$\underline{\nabla} \cdot \underline{B} = 0 \quad (3)$$

$$\underline{\nabla} \times \underline{B} = \frac{4\pi}{c} \underline{J} \quad (4)$$

and $\underline{J} \equiv 0$ in the vacuum.

Here we use Gaussian units and neglect the displacement current, since electric current changes are assumed slow.

In the region containing plasma or conductors, the material satisfies the usual magnetohydrodynamic equations. We shall assume the plasma is everywhere sufficiently dense so that quasineutrality will hold. Then we can write these equations

$$\frac{\partial \rho}{\partial t} + \underline{\nabla} \cdot \rho \underline{v} = 0 \quad (5)$$

$$\rho \frac{d\underline{v}}{dt} + \underline{\nabla} nkT = \frac{1}{c} \underline{J} \times \underline{B} + \mu \nabla^2 \underline{v} \quad (6)$$

$$\underline{E} + \frac{1}{c} \underline{v} \times \underline{B} = \eta \underline{J} \quad (7)$$

$$nk \frac{\partial T}{\partial t} + nk \underline{\nabla} \cdot T \underline{v} = (2-\gamma) nkT \underline{\nabla} \cdot \underline{v} + h \nabla^2 T + \eta J^2 + \mu \nabla v : \nabla v \quad (8)$$

Where both viscosity and thermal conductivity will be important if the plasma is sufficiently hot.

The equations (1-8) represent the complete mathematical problem we would like to solve. However, we must simplify them considerably in order to make the problem tractable computationally.

We shall assume the dominant magnetic field arises from the current in the external conductors, the next order from the toroidal plasma currents. Thus we write the magnetic field in terms of a vector potential

$$\underline{B} = \underline{\nabla} \times \underline{A} \quad (9)$$

and assume that \underline{A} has only a toroidal component, plus a contribution due to the toroidal magnetic field. Since the magnetic potential has only one component, we replace it by a scalar potential ψ , defined by

$$\underline{B} = e_{\varphi} B_{\varphi} + \frac{e_{\varphi}}{2\pi r} \times \underline{\nabla} \psi \quad (10)$$

where the (r, φ, z) coordinate system has φ in the toroidal direction, r the distance from the major axis, z the position relative to the midplane of the system, and B_{φ} is of the form $2I_0/10r$ initially.

Combining Eqs. 2, 4 and 7, the magnetic field is found to satisfy

$$\frac{\partial \underline{B}}{\partial t} - \underline{\nabla} \times (\underline{V} \times \underline{B}) = \frac{c^2}{4\pi} \underline{\nabla} \times \eta \underline{\nabla} \times \underline{B}. \quad (11)$$

After the use of several vector identities and the approximation that the plasma current contributing to the magnetic field flows in the toroidal direction, this can be rewritten

$$\frac{\partial \underline{B}}{\partial t} + \underline{\nabla} \cdot (\underline{V} \underline{B}) = \frac{\eta c^2}{4\pi} \nabla^2 \underline{B} + \underline{B} \cdot \underline{\nabla} \underline{V} \quad (12)$$

This has the form of a conservation equation with diffusion. The last term represents the Ware pinch.¹ This equation can also be cast in the form of a diffusion equation in ψ , by substituting Eq. (10) into it.

The complete mathematical statement of this problem is now Eqs. (5) and (12) as written, and Eqs. (6) and (8) with \underline{J} eliminated in terms of \underline{B} . This is one conservation equation for ρ and three convection plus diffusion equations for \underline{V} , \underline{B} and T . They are to be solved in a coordinate system determined by \underline{B} . The remainder of this report is a description of the mechanics of that coordinate calculation.

GEOMETRODYNAMICS

The magnetic field which is the solution of Eq. (12) forms a set of magnetic surfaces, whose locations may most easily be determined through examination of the values of ψ in Eq. (10). By construction, the components of \underline{B} in the (r, z) plane lie along constant ψ surfaces.

For the problems of interest to us, these are multiply-connected, as in Fig. 2. The choice of coordinate system becomes very important in such a geometry. Heat and material flow is very rapid along \underline{B} ; much slower across it. Thus one coordinate should be along the magnetic surfaces. The flux ψ is the natural coordinate across them. The breaking of the volume into basic computational cells is difficult because of the presence of irregular points and surfaces, such as the magnetic axes and separatrix.

We choose to break the volume into triangular elements so that our mesh does not force a spurious structure on the problem. We use methods which have been developed previously for hydrodynamics² and magnetohydrodynamics³. Our basic cells move in the (r, z) plane, and the plasma dynamics are calculated by interpreting the equations of motion in the Lagrangian frame of these cells. Within each time advance, an iteration is performed to locate the cells, then physical quantities are transported among the cells.

The Lagrangian pressure-balance model is applied only to the ideal dissipation-free pressure and the $\underline{J} \times \underline{B}$ forces (including both the toroidal and poloidal magnetic fields). The mass in a cell, the

adiabatic constant and the magnetic flux in the cell are all held constant as the vertices are adjusted in position in response to force imbalance. The degree of adjustment is directly proportional to the strength of the force imbalance.

The iterative scheme used to achieve force balance is a two-dimensional Newton-Raphson method. The pressure gradient force, the $\underline{J} \times \underline{B}$ forces and the corresponding derivatives are calculated at each vertex within the plasma. The vertices are then moved in response to those forces while conserving the mass and magnetic flux in a cell and the adiabatic constant.

Figure 3 illustrates the basic structure of the triangular grid. If each vertex is joined with the bisecting point on the opposite side, then these lines form a closed region about each vertex as shown. This region forms the basic cell for the numerical grid. The pressure, number densities, temperatures and toroidal field flux are defined at these vertices and assumed constant throughout the cell. The toroidal current and poloidal field flux are defined on the triangle sides.

The $\nabla \cdot \underline{B} = 0$ condition on the poloidal field and the $\nabla \cdot \underline{J} = 0$ condition on the poloidal current are identically satisfied by summing the corresponding magnetic and current fluxes around the triangle sides. In the vacuum regions the magnetic field fluxes are iterated to $\underline{J} = 0$ while $\nabla \cdot \underline{B} = 0$.

MAGNETOHYDRODYNAMICS

Once the vertex positions have been determined to the required degree of convergence, the poloidal and toroidal magnetic diffusion is determined from Faraday's law and the magnetic fluxes are integrated forward in time. The particle and energy transport are then calculated, the time step updated, and the force balance iteration begins anew.

To determine the grad p force at a vertex, we find the pressure gradient on a triangle side common to two triangles,

assuming the pressure is constant throughout each triangle. (See Figure 4.) The pressure in a triangle is defined to be the average of the pressure at each vertex; i.e.,

$$\langle p \rangle_1 = 1/3 (p_1 + p_2 + p_3).$$

The volume averaged force is given by

$$\underline{F} = \int \nabla p dV,$$

and assuming a discrete pressure difference across some thickness $\delta\tau$, we have

$$\underline{F} = 1/3 (p_4 - p_1) 2\pi \langle r \rangle \ell \delta\tau^{\wedge},$$

where $\delta\tau^{\wedge}$ is normal to the triangle side, and ℓ is the length of the triangle side. The (r, z) components of the force at the vertices at the ends of the side ℓ are then

$$F_r = 1/6 (p_4 - p_1) 2\pi \langle r \rangle (z_2 - z_3),$$

$$F_z = 1/6 (p_4 - p_1) 2\pi \langle r \rangle (r_2 - r_3).$$

The pressure gradient force is determined and summed at every plasma vertex in a similar manner.

Note that since the pressure gradient is calculated as a discrete jump across a triangle side (assuming the pressure is constant in each triangle adjoining that side) if a pressure variation appears on a flux surface, the system responds very slowly to this variation. As a result, the convergence to force balance is much slower along a flux surface than across a flux surface.

This difficulty is removed by employing a conservative pressure-smoothing routine on the plasma flux surfaces. This is used only when the plasma has ceased to compress (or expand); otherwise, the iteration would be unstable. The pressure variation on a flux surface, with the pressure smoothing in effect, is generally of the

order of 1% and the algorithm converges. If the pressure is smoothed on a flux surface there is a corresponding adiabatic change in the temperature.

The primary poloidal flux variable is $\delta\psi_i$, which is the poloidal flux through the i^{th} triangle side and is equal to the difference in the poloidal flux function between adjacent vertices. Summing the $\delta\psi_i$ around the triangle sides assures that the $\nabla \cdot \underline{B} = 0$ condition is identically satisfied.

The magnetic field is given by Eq. (10) and from Figure 5, the r and z -components of the poloidal field for triangle number one are then

$$B_{r_1} = - \frac{[(r_2 - r_3) \delta\psi_1 - (r_1 - r_3) \delta\psi_2]}{4\pi \langle r_1 \rangle A_1}$$

$$B_{z_1} = - \frac{[(z_2 - z_3) \delta\psi_1 - (z_1 - z_3) \delta\psi_2]}{4\pi \langle r_1 \rangle A_1},$$

where A_1 is the area of the triangle. These fields are assumed to be constant throughout the triangle.

The toroidal currents are determined from the integral form of Ampère's law. The poloidal field is assumed constant inside a triangle and the toroidal current flowing on a triangle side is due to changes in the tangential field across the boundaries. Starting with Ampère's law and from Figure 6,

$$\begin{aligned} I &= \frac{c}{4\pi} \oint \underline{B} \cdot d\underline{\ell} \\ &= \frac{c}{4\pi} [B_{r_1} (r_1 - r_2) + B_{z_1} (z_1 - z_2) + B_{r_2} (r_2 - r_1) \\ &\quad + B_{z_2} (z_2 - z_1)] \\ &= \frac{c}{4\pi} [\Delta B_r \Delta r + \Delta B_z \Delta z], \end{aligned}$$

and the current density is then

$$\underline{j} = \frac{I \hat{n}}{A},$$

where $A = \ell \delta \tau$ and \hat{n} is the unit vector in the toroidal direction.

The poloidal $\underline{j} \times \underline{B}$ force on a triangle side is then given by

$$\begin{aligned} \underline{F} &= \frac{1}{c} \int \underline{j} \times \underline{B} \, dV \\ &= \frac{1}{2} (\Delta B_r \Delta r + \Delta B_z \Delta z) \langle r \rangle (\hat{n} \times \langle \underline{B} \rangle), \end{aligned}$$

where $\langle \underline{B} \rangle$ is the average poloidal field at the mid-point of the side and the force on each vertex is one-half of the above quantity.

The toroidal field (B_θ) is stored as a cell-centered flux which is independent of the toroidal coordinate and thus divergence free. The poloidal current flux through the triangle sides is determined from Ampère's law

$$\begin{aligned} I &= \frac{c}{4\pi} \oint \underline{B} \cdot d\underline{\ell}, \\ &= \frac{c}{4\pi} \Delta \langle B_\theta \rangle \langle r \rangle \Delta \theta, \end{aligned}$$

where $\Delta \langle B_\theta \rangle$ is the jump in the average toroidal field and the average field is given by

$$\langle B_\theta \rangle = \frac{1}{3} \sum_{i=1}^3 B_{\theta i},$$

and thus

$$\underline{j} = \frac{I \hat{n}}{A} = \frac{c}{4\pi} \frac{\Delta \langle B_\theta \rangle \langle r \rangle \Delta \theta}{\langle r \rangle \Delta \theta \delta \tau}$$

The volume weighted $\underline{j} \times \underline{B}$ force on a triangle side due to the toroidal field is then

$$\begin{aligned} \underline{F} &= \frac{1}{c} \int \underline{j} \times \underline{B} \, dV \\ &= \frac{1}{2} [\langle r \rangle_{\tau} B_{\theta_{\tau}}] \overline{\langle r \rangle_{\tau} B_{\theta_{\tau}}} \frac{\ell}{\langle r \rangle_s} \hat{n}_{\perp}, \end{aligned}$$

where

$$\langle r \rangle_s = \frac{1}{2} (r_i + r_j),$$

and

$$\langle r \rangle_{\tau} \equiv \sum_{i=1}^3 1/\left(\frac{1}{r_i}\right),$$

with

$$[\langle r \rangle_{\tau} B_{\theta_{\tau}}] \equiv \langle r \rangle_{\tau_i} B_{\theta_{\tau_i}} - \langle r \rangle_{\tau_j} B_{\theta_{\tau_j}}$$

and

$$\overline{\langle r \rangle_{\tau} B_{\theta_{\tau}}} \equiv \frac{1}{2} [\langle r \rangle_{\tau_i} B_{\theta_{\tau_i}} + \langle r \rangle_{\tau_j} B_{\theta_{\tau_j}}].$$

All the forces have now been determined at the vertices, so the vertices can be moved in response to those forces. The vacuum grid positions are then iterated to find locations giving approximately equal areas in the vacuum region. Once the new positions have been computed throughout the grid, the new side lengths, weighting factors, triangle areas and volumes are determined. Then the vacuum field is iterated to $\nabla \times \underline{B} = 0$ and the toroidal field is made divergence free while conserving flux. If the plasma has not yet reached force-balance, the new densities, pressure and temperatures are determined adiabatically ($pV^{\gamma} = \text{constant}$) and subsequent passes are made through the iteration loop until equilibrium is reached.

INITIAL CONDITIONS

The initial equilibrium position is determined with no toroidal magnetic field. This is because the toroidal field is the dominant field component and the convergence from the initial conditions to the initial equilibrium state is an extremely slow process in the full equations. Once the initial equilibrium state is reached, the toroidal and vertical fields are initialized and the time evolution begins.

The iteration normally converges reasonably quickly except for low plasma pressure cases ($\beta_p \ll 1$). Under these conditions the $\underline{j} \times \underline{B}$ forces overwhelm the pressure force and the iteration to force balance becomes unstable.

The correction to this problem is to include viscosity in the basic iteration to smooth the vertex motion. The viscosity may be viewed as a force which moves vertices apart if the length of a triangle side on a flux surface becomes significantly less than the average length of the sides comprising that flux surface. This viscosity is very important, and helps force the system to equilibrium relatively rapidly.

The approach to equilibrium proceeds in three quasi-independent steps. First, the change in a vertex position approaches zero exhibiting $\nabla p = 1/c \underline{j} \times \underline{B}$ force balance locally. Second, the average length of a triangle side making up a flux surface approaches a constant indicating the system has reached equilibrium globally. Third, the pressure on a flux surface approaches a constant (at a very slow rate).

Since the approach to constant pressure on a flux surface is a very slow process, a conservative pressure-smoothing algorithm is employed to enhance the approach to equilibrium. This routine is not employed until the average length $\langle \ell \rangle$ of the triangle sides making up each plasma flux surface has reached a constant so as not to destroy convergence. The system is declared to have reached a steady state only when (1) the maximum change in any plasma vertex position $(\Delta r / \Delta r_{init}, \Delta z / \Delta z_{init})$ is $\sim O(10^{-5} \text{ cm})$,

(2) the average length of a triangle side on each plasma flux surface has reached a constant value and (3), the pressure variation on a plasma surface is less than 1.5 - 2%. With the toroidal field off, the system reaches equilibrium after about 100 iterations with $\beta \sim 1$ and after about 130 iterations with $\beta \ll 1$. Table I illustrates several parameters associated with convergence for the same initial conditions with and without pressure smoothing after 160 iterations.

TRANSPORT

Once the initial steady state geometry has been reached, the toroidal field and any vertical fields are applied and the physical dynamics begin with the diffusion of the magnetic fields accounted for at every time step.

The system is iterated to force balance, in the same manner as discussed above, at every time step. Once force balance is reached the magnetic fields are determined in the plasma and conductors and integrated forward in time with a time step determined from the plasma conductivity.

The magnetic diffusion for the poloidal and toroidal fields are treated separately. In each case the electric fields are determined algebraically from Ohm's law $\underline{E} = \underline{J}/\sigma$. For the plasma, σ is the Spitzer conductivity which is determined at every vertex as a function of the temperature and density at that vertex. The code has provisions to account for anomalous effects. Once the electric fields have been determined, the magnetic diffusion is calculated from the integral form of Faraday's law.

To determine the diffusion of the poloidal magnetic field, the toroidal electric field is calculated at all plasma vertices. First, the current and area-weighted conductivity are summed on each plasma flux surface

$$I_s = \sum_{j=1}^n I_j,$$

and

$$\sigma_s = \sum_{j=1}^n \frac{\sigma_j A_j}{r_j},$$

where the sum is over the number of vertices comprising the flux surface. The toroidal electric field at each vertex is then given by

$$E_{\theta i} = \frac{I_s}{\sigma_s r_i}.$$

From Faraday's law

$$\frac{d\delta\psi}{dt} = -c \oint \underline{E} \cdot d\underline{\ell},$$

with the path of integration around the basic cell, the new poloidal flux through a triangle side is given by

$$\delta\psi_{i+\frac{1}{2}}^{\text{new}} = \delta\psi_{i+\frac{1}{2}}^{\text{old}} - 2\pi c \Delta t [E_{\theta i+1} r_{i+1} - E_{\theta i} r_i].$$

The poloidal electric field on a triangle side is given by

$$E = j/\sigma$$

$$E_{i+\frac{1}{2}} = \frac{c}{4\pi} [r_i \phi_i / A_i - r_{i+1} \phi_{i+1} / A_{i+1}] / \sigma_{i+\frac{1}{2}}$$

where ϕ_i is the toroidal magnetic flux at vertex i . The new toroidal flux is then

$$\phi_i^{\text{new}} = \phi_i^{\text{old}} - 2\pi c \Delta t (\underline{\nabla} \times \underline{E}_{i+\frac{1}{2}}).$$

Once the magnetic field diffusion has been calculated, the code accounts for particle and energy transport both parallel and perpendicular to the magnetic field. (These routines are still in the testing stage.) The flow velocities may be calculated from the momentum equation and Ohm's law, and the mass and temperature are transported. The model does not presently include internal sinks (a limiter in the

divertor) so the transport leaves p and T constant on flux surfaces, and diffuses them across flux surfaces. This completes the algorithm. The time is then updated and the new time step is calculated as a fraction of the resistive diffusion timescale. The system is then iterated to a new equilibrium position.

With the toroidal field taken into account, the plasma reaches force balance after 10-20 iterations. More iterations are required at the first time step.

Both the approach to the initial equilibrium state and the time evolution have a built-in check-point restart. Thus the system variables are backed up onto disk at frequent intervals and a continual check is made on the convergence rate to equilibrium. If, for any reason, the system ceases to converge properly, the program is halted; and after the appropriate corrections are made it can be restarted. This also serves as a protection mechanism for computer system crashes.

SUMMARY AND CONCLUSIONS

The work presented here is an outgrowth of the dynamic MHD Linus 2 project⁴. The code is used to calculate the time evolution of a finite conductivity plasma in an arbitrary shaped, finite-conductivity vessel. The model is unique in that it follows both the resistive diffusion and dynamical evolution of the plasma in an arbitrary geometry. Since the poloidal electrostatic field is calculated, its role in the evolution of trapped electrons can be determined. The flexibility of the triangular grid geometry permits an investigation of non-circular tokamaks including Doublet and divertor systems.

With the addition of the check-point restart and the self-consistent tests governing the approach to equilibrium, the code is essentially self-sufficient. Once a reasonable choice of initial conditions is made (plasma size, geometry, density and temperature;

toroidal current and field strength), no further input is required from the user.

The introduction of viscosity and pressure smoothing on a flux surface admits to an investigation of low beta systems with as equal a facility as high beta ($\beta_p \sim 1$) systems for which the code was originally designed. The code is now undergoing thorough testing by investigating the outward movement (toward the limiter) of the plasma flux surfaces as β_p is increased from a very small value to a value of order one. These results are expected in the near future. Future scheduled research includes general thermal and particle transport in Doublet and divertor systems.

REFERENCES

1. R. D. Hazeltine, A. A. Ware, D. J. Sigmar, S. P. Hirshman, J. E. McCune, E. C. Crume, J. T. Hogan and J. F. Clarke, Plasma Physics and Controlled Nuclear Fusion Research, 1974, IAEA-CN-33, p. 589.
2. M. J. Fritts and J. P. Boris, NRL Memorandum Report No. 3446 (Feb. 1977).
3. J. H. Gardner and J. P. Boris, NRL Memorandum Report No. 3152 (Nov. 1975).
4. J. P. Boris and K. L. Hain, Bull. Am. Phys. Soc., paper 6G1, p. 942 (October 1974).

Table 1.

Initial Conditions: $T = 0.1 \text{ keV}$, $n = 1.3 \times 10^{13}$, $I = 70\text{KA}$.

<u>Flux Surface</u>	<u>$\Delta p(\%)$</u>	<u>Without Smoothing</u>	
		<u>$\langle \ell \rangle (\text{cm})$</u>	<u>$\max \Delta r, \Delta z (\text{cm})$</u>
1			$2.4 \times 10^{-5}, 3.7 \times 10^{-6}$
2	4.4	.660	$3.1 \times 10^{-5}, 3.3 \times 10^{-6}$
3	8.1	1.649	$3.1 \times 10^{-5}, 6.9 \times 10^{-6}$
4	35.3	1.575	$2.8 \times 10^{-5}, 2.3 \times 10^{-5}$
5	15.9	2.715	$2.6 \times 10^{-5}, 1.8 \times 10^{-5}$

<u>Flux Surface</u>	<u>$\Delta p(\%)$</u>	<u>With Smoothing</u>	
		<u>$\langle \ell \rangle (\text{cm})$</u>	<u>$\max \Delta r, \Delta z (\text{cm})$</u>
1			$2.7 \times 10^{-5}, 4.5 \times 10^{-7}$
2	1.5	.667	$4.3 \times 10^{-5}, 2.1 \times 10^{-5}$
3	<1.	1.668	$4.3 \times 10^{-5}, 1.5 \times 10^{-5}$
4	1.1	1.590	$5.3 \times 10^{-5}, 7.7 \times 10^{-5}$
5	<1.	2.731	$4.7 \times 10^{-5}, 4.9 \times 10^{-5}$

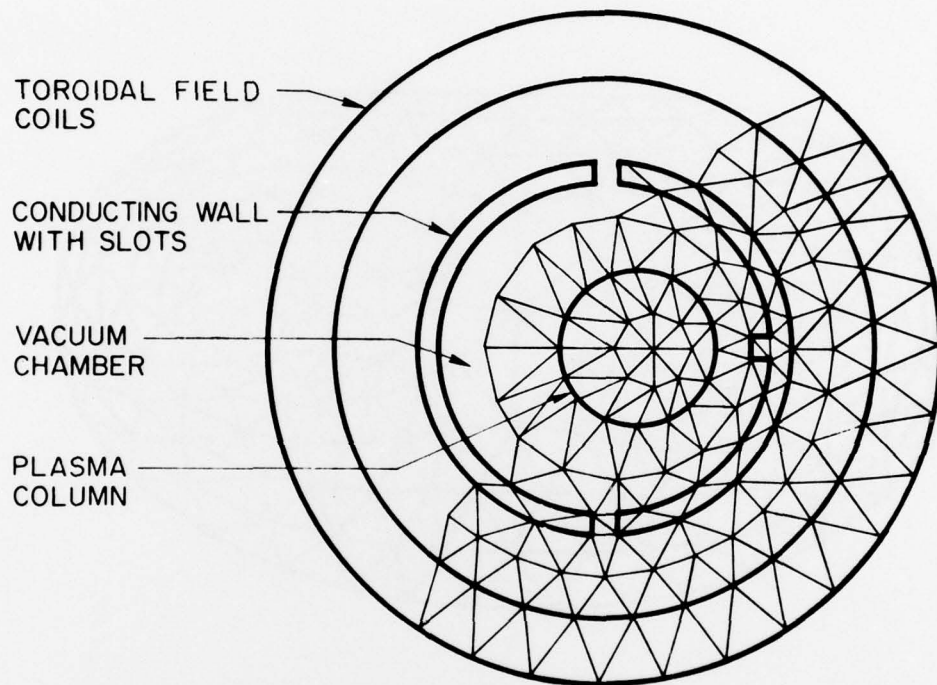


Fig. 1 - Application of triangular gridding to a typical tokamak configuration. Plasma and vacuum regions are represented as well as conducting parts such as field coils, conducting wall and limiter.

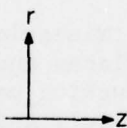
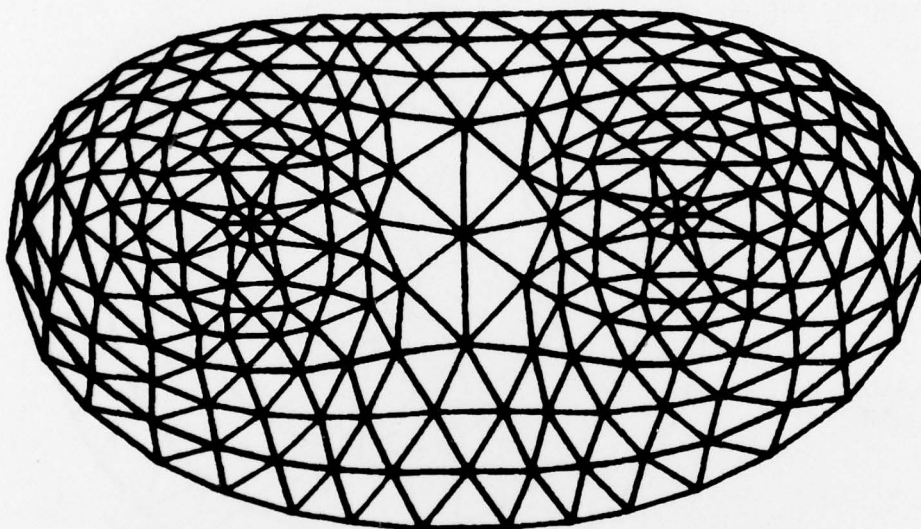
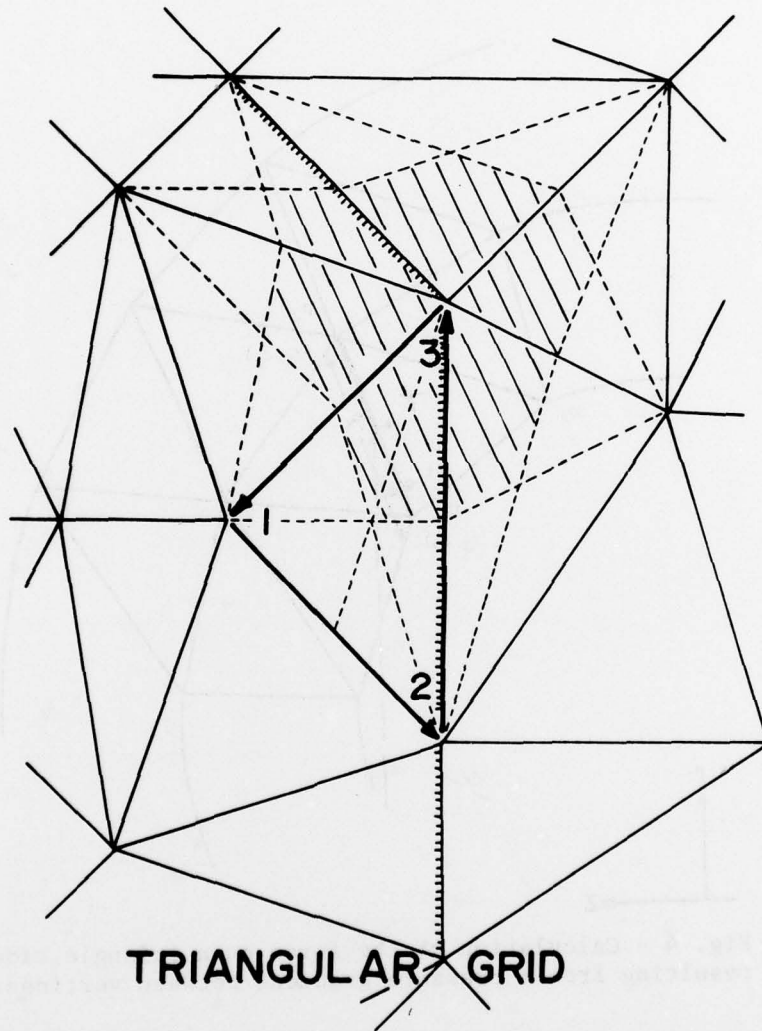


Fig. 2 - Tessalation of the magnetic surfaces in a doublet configuration. Note the finer grid near the two magnetic axes and on the outside in the regions where trapped-particle and ballooning modes are expected.



TRIANGULAR GRID

Fig. 3 - Detail of triangular-grid elements. A triangle is made up of three directed line segments, and a vertex represents the (shaded) region defined by the center of mass of each surrounding triangle and the midpoint of each side.

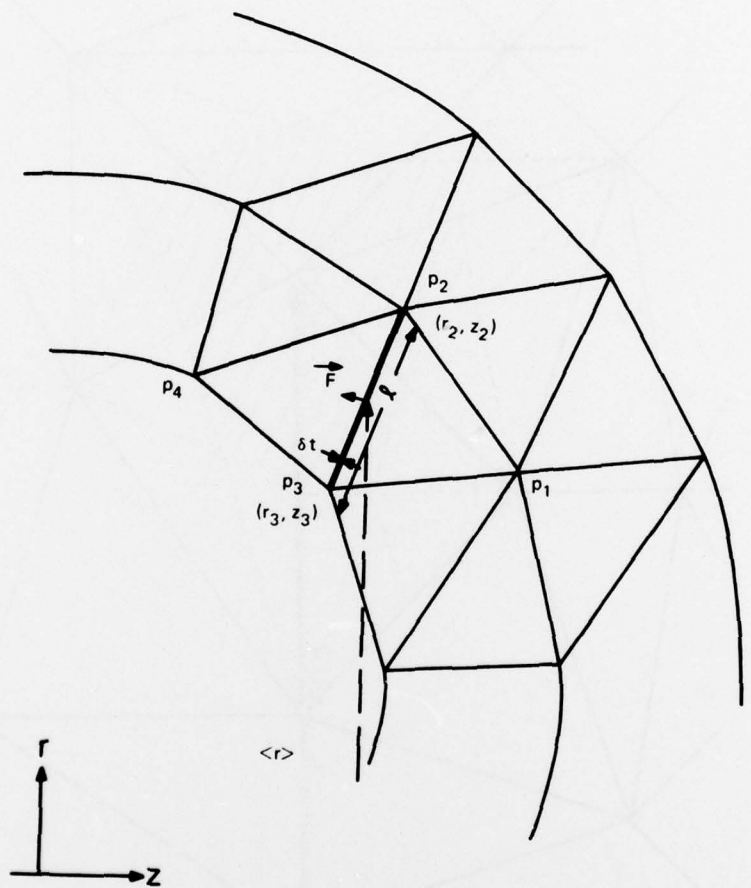


Fig. 4 - Calculation of the force on a triangle side resulting from a pressure gradient between vertices.

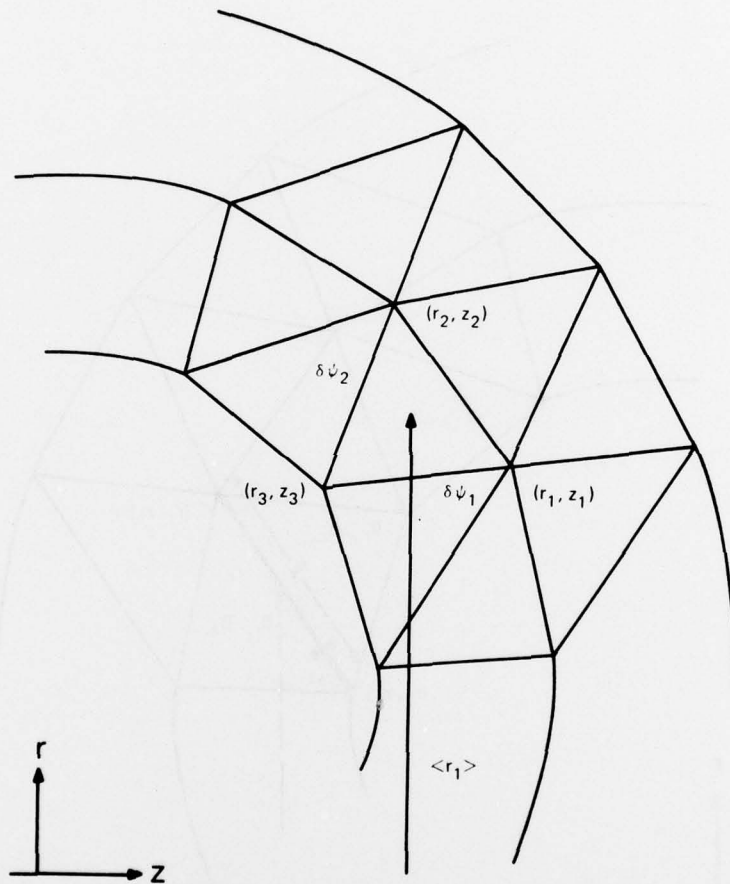


Fig. 5 - Calculation of poloidal magnetic field in a triangle resulting from the poloidal fluxes through the sides. Circular curves represent flux surfaces.

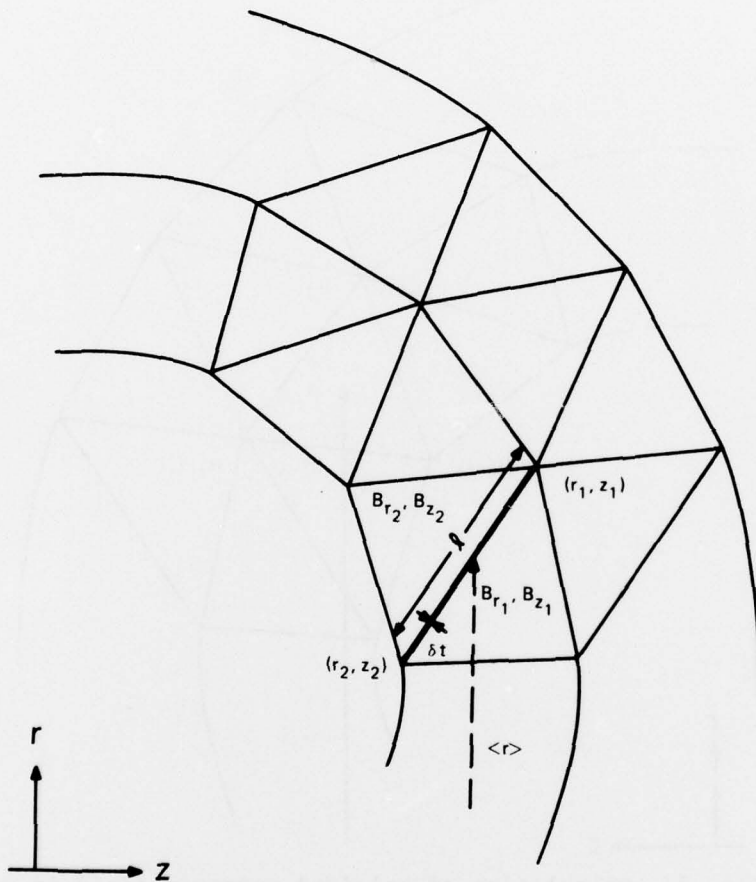


Fig. 6 - Calculation of $J \times B$ force on an edge resulting from magnetic field gradient between triangles.